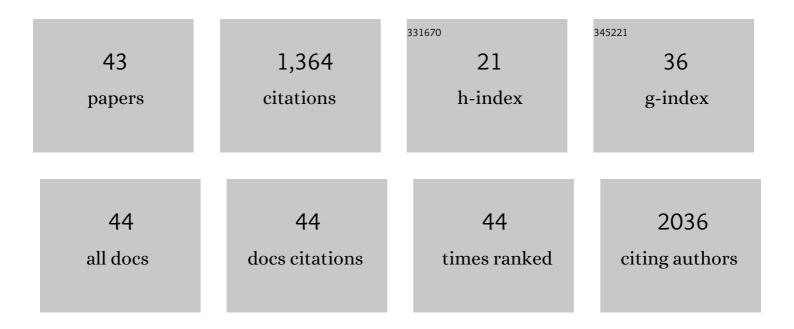
Alexandre Cochet

List of Publications by Year in descending order

Source: https://exaly.com/author-pdf/10495694/publications.pdf Version: 2024-02-01



#	Article	IF	CITATIONS
1	[18F]FDG-PET predicts complete pathological response of breast cancer to neoadjuvant chemotherapy. European Journal of Nuclear Medicine and Molecular Imaging, 2007, 34, 1915-1924.	6.4	160
2	In Newly Diagnosed Diffuse Large B-Cell Lymphoma, Determination of Bone Marrow Involvement with ¹⁸ F-FDG PET/CT Provides Better Diagnostic Performance and Prognostic Stratification Than Does Biopsy. Journal of Nuclear Medicine, 2013, 54, 1244-1250.	5.0	156
3	Baseline metabolic tumour volume is an independent prognostic factor in Hodgkin lymphoma. European Journal of Nuclear Medicine and Molecular Imaging, 2014, 41, 1735-1743.	6.4	152
4	Influence of Software Tool and Methodological Aspects of Total Metabolic Tumor Volume Calculation on Baseline [18F]FDG PET to Predict Survival in Hodgkin Lymphoma. PLoS ONE, 2015, 10, e0140830.	2.5	90
5	18F-FDG PET/CT provides powerful prognostic stratification in the primary staging of large breast cancer when compared with conventional explorations. European Journal of Nuclear Medicine and Molecular Imaging, 2014, 41, 428-437.	6.4	67
6	HER2-positive breast cancer: 18F-FDG PET for early prediction of response to trastuzumab plus taxane-based neoadjuvant chemotherapy. European Journal of Nuclear Medicine and Molecular Imaging, 2014, 41, 1525-1533.	6.4	57
7	Prognostic relevance at 5Âyears of the early monitoring of neoadjuvant chemotherapy using 18F-FDG PET in luminal HER2-negative breast cancer. European Journal of Nuclear Medicine and Molecular Imaging, 2014, 41, 416-427.	6.4	54
8	Evaluation of Breast Tumor Blood Flow with Dynamic First-Pass ¹⁸ F-FDG PET/CT: Comparison with Angiogenesis Markers and Prognostic Factors. Journal of Nuclear Medicine, 2012, 53, 512-520.	5.0	53
9	Role of Positron Emission Tomography for the Monitoring of Response to Therapy in Breast Cancer. Oncologist, 2015, 20, 94-104.	3.7	53
10	Identification of Biomarkers Including 18FDG-PET/CT for Early Prediction of Response to Neoadjuvant Chemotherapy in Triple-Negative Breast Cancer. Clinical Cancer Research, 2015, 21, 5460-5468.	7.0	46
11	Emidec: A Database Usable for the Automatic Evaluation of Myocardial Infarction from Delayed-Enhancement Cardiac MRI. Data, 2020, 5, 89.	2.3	46
12	Salvage extended field or involved field nodal irradiation in 18F-fluorocholine PET/CT oligorecurrent nodal failures from prostate cancer. European Journal of Nuclear Medicine and Molecular Imaging, 2019, 46, 40-48.	6.4	41
13	Pattern of occult nodal relapse diagnosed with 18F-fluoro-choline PET/CT in prostate cancer patients with biochemical failure after prostate-only radiotherapy. Radiotherapy and Oncology, 2014, 111, 120-125.	0.6	34
14	The extent of myocardial damage assessed by contrast-enhanced MRI is a major determinant of N-BNP concentration after myocardial infarction. European Journal of Heart Failure, 2004, 6, 555-560.	7.1	30
15	Nonsupervised Ranking of Different Segmentation Approaches: Application to the Estimation of the Left Ventricular Ejection Fraction From Cardiac Cine MRI Sequences. IEEE Transactions on Medical Imaging, 2012, 31, 1651-1660.	8.9	27
16	18F-FDG PET–Derived Tumor Blood Flow Changes After 1 Cycle of Neoadjuvant Chemotherapy Predicts Outcome in Triple-Negative Breast Cancer. Journal of Nuclear Medicine, 2016, 57, 1707-1712.	5.0	27
17	Breast Cancer Blood Flow and Metabolism on Dual-Acquisition ¹⁸ F-FDG PET: Correlation with Tumor Phenotype and Neoadjuvant Chemotherapy Response. Journal of Nuclear Medicine, 2018, 59, 1035-1041.	5.0	27
18	Visual estimation of the global myocardial extent of hyperenhancement on delayed contrast-enhanced MRI. European Radiology, 2004, 14, 2182-2187.	4.5	26

#	Article	IF	CITATIONS
19	Relationship Between Fragmented QRS and No-Reflow, Infarct Size, and Peri-Infarct Zone Assessed Using Cardiac Magnetic Resonance in Patients With Myocardial Infarction. Canadian Journal of Cardiology, 2014, 30, 204-210.	1.7	26
20	Tumor Volume and Metabolism of Prostate Cancer Determined by Proton Magnetic Resonance Spectroscopic Imaging at 3T Without Endorectal Coil Reveal Potential Clinical Implications in the Context of Radiation Oncology. International Journal of Radiation Oncology Biology Physics, 2011, 80, 1087-1094.	0.8	22
21	Current role of multiparametric magnetic resonance imaging for prostate cancer. Quantitative Imaging in Medicine and Surgery, 2015, 5, 754-64.	2.0	21
22	Prognostic Value of Microvascular Damage Determined by Cardiac Magnetic Resonance in Non ST-Segment Elevation Myocardial Infarction. Investigative Radiology, 2010, 45, 725-732.	6.2	17
23	FDG PET/CT for prognostic stratification of patients with metastatic breast cancer treated with first line systemic therapy: Comparison of EORTC criteria and PERCIST. PLoS ONE, 2018, 13, e0199529.	2.5	15
24	Utility of Cardiac Magnetic Resonance to assess association between admission hyperglycemia and myocardial damage in patients with reperfused ST-Segment Elevation Myocardial Infarction. Journal of Cardiovascular Magnetic Resonance, 2008, 10, 2.	3.3	13
25	Combination of breast imaging parameters obtained from 18F-FDG PET and CT scan can improve the prediction of breast-conserving surgery after neoadjuvant chemotherapy in luminal/HER2-negative breast cancer. European Journal of Radiology, 2019, 113, 81-88.	2.6	13
26	Improved Estimation of Cardiac Function Parameters Using a Combination of Independent Automated Segmentation Results in Cardiovascular Magnetic Resonance Imaging. PLoS ONE, 2015, 10, e0135715.	2.5	11
27	Biological correlates of tumor perfusion and its heterogeneity in newly diagnosed breast cancer using dynamic first-pass 18F-FDG PET/CT. European Journal of Nuclear Medicine and Molecular Imaging, 2020, 47, 1103-1115.	6.4	11
28	Unusual uptakes on 18F-fluorocholine positron emission tomography/computed tomography (PET/CT): a retrospective study of 368 prostate cancer patients referred for a biochemical recurrence or an initial staging. Quantitative Imaging in Medicine and Surgery, 2021, 11, 172-182.	2.0	11
29	Relation between high levels of myeloperoxidase in the culprit artery and microvascular obstruction, infarct size and reverse remodeling in ST-elevation myocardial infarction. PLoS ONE, 2017, 12, e0179929.	2.5	10
30	Myocardial Infarction Quantification from Late Gadolinium Enhancement MRI Using Top-Hat Transforms and Neural Networks. Algorithms, 2021, 14, 249.	2.1	9
31	Clinical value of CA 15-3 for detection of distant metastases in newly diagnosed breast cancer. Annales De Biologie Clinique, 2017, 75, 421-429.	0.1	7
32	Automatic Fuzzy Classification of the Washout Curves From Magnetic Resonance First-Pass Perfusion Imaging After Myocardial Infarction. Investigative Radiology, 2005, 40, 545-555.	6.2	6
33	Positron Emission Tomography and Neoadjuvant Therapy of Breast Cancer. Journal of the National Cancer Institute Monographs, 2011, 2011, 111-115.	2.1	6
34	Three-dimensional nuclear magnetic resonance spectroscopy: a complementary tool to multiparametric magnetic resonance imaging in the identification of aggressive prostate cancer at 3.0T. Quantitative Imaging in Medicine and Surgery, 2021, 11, 3749-3766.	2.0	4
35	Comparison of different segmentation approaches without using gold standard. Application to the estimation of the left ventricle ejection fraction from cardiac cine MRI sequences. , 2011, 2011, 2663-6.		3
36	Factor analysis-based approach for early uptake automatic quantification of breast cancer by 18F-FDG PET images sequence. Biomedical Signal Processing and Control, 2014, 9, 19-31.	5.7	3

ALEXANDRE COCHET

#	Article	IF	CITATIONS
37	Comparison of two techniques (in vivo and ex-vivo) for evaluating the elastic properties of the ascending aorta: Prospective cohort study. PLoS ONE, 2021, 16, e0256278.	2.5	3
38	Detection of Myocardial Infarction by Cardiac Magnetic Resonance in Embolic Stroke Related to First Diagnosed Atrial Fibrillation. Journal of Stroke and Cerebrovascular Diseases, 2021, 30, 105753.	1.6	2
39	Comparison between tumour metabolism derived from 18F-FDG PET/CT and accurate cytogenetic stratification in newly diagnosed multiple myeloma patients. Quantitative Imaging in Medicine and Surgery, 2021, 11, 4299-4309.	2.0	2
40	Reply: Semiquantification Limitations: FMTVDM ^{©â,,—} Demonstrates Quantified Tumor Response to Treatment with Both Regional Blood Flow and Metabolic Changes. Journal of Nuclear Medicine, 2018, 59, 1644-1644.	5.0	1
41	Impact of ascending aorta replacement by graft on elastic properties of descending thoracic aorta evaluated by cardiac magnetic resonance imaging. Magnetic Resonance Materials in Physics, Biology, and Medicine, 2020, 33, 641-647.	2.0	1
42	Reply: Prognostic Implications of Imaging-Based Bone Marrow Assessment in Lymphoma: ¹⁸ F-FDG PET, MR Imaging, or ¹⁸ F-FDG PET/MR Imaging?. Journal of Nuclear Medicine, 2013, 54, 2018.1-2018.	5.0	0
43	MR spectroscopy compared with DW-MRI and DCE-MRI at 3-tesla for the noninvasive prediction of short-term radiation response for patients with localized prostate cancer Journal of Clinical Oncology, 2012, 30, 122-122.	1.6	Ο